ACSNANO
www.acsnano.org
ARTICLE

Top-Contact Self-Aligned Printing for High-Performance Carbon Nanotube Thin-Film Transistors with Sub-Micron Channel Length

Xuan Cao,[†,§] Fanqi Wu,[†,§] Christian Lau,[‡] Yihang Liu,[‡] Qingzhou Liu,[†] and Chongwu Zhou*[,†,‡]

[†]Department of Materials Science and [‡]Department of Electrical Engineering, University of Southern California, Los Angeles, California 90089, United States

Supporting Information

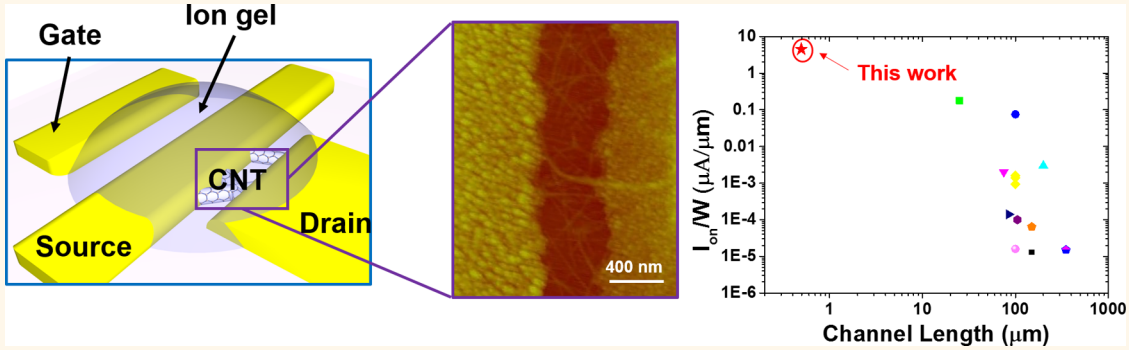

ABSTRACT: **Semiconducting single-wall carbon nanotubes are ideal semiconductors for printed thin-film transistors due to their excellent electrical performance and intrinsic printability with solution-based deposition. However, limited by resolution and registration accuracy of current printing techniques, previously reported fully printed nanotube transistors had rather long channel lengths (>20 μm) and consequently low current-drive capabilities (<0.2 μA/μm). Here we report fully inkjet printed nanotube transistors with dramatically enhanced on-state current density of ~4.5 μA/μm by downscaling the devices to a sub-micron channel length with top-contact self-aligned printing and employing high-capacitance ion gel as the gate dielectric. Also, the printed transistors exhibited a high on/off ratio of ~10^5, low-voltage operation, and good mobility of ~15.03 cm^2 V^{-1}s^{-1}. These advantageous features of our printed transistors are very promising for future high-definition printed displays and sensing systems, low-power consumer electronics, and large-scale integration of printed electronics.**

KEYWORDS: *single-wall carbon nanotubes, ultrashort-channel thin-film transistors, top-contact self-aligned printing, on-state current density*

Semiconducting single-wall carbon nanotubes (SWCNTs) have been gaining attention in developing fully printed thin-film transistors (TFTs) due to their outstanding electric and mechanical properties, solution-based low-temperature deposition process, and stability against oxygen and moisture.[1−6] Main-stream printing technologies such as inkjet printing,[7,8] aerosol-jet printing,[9−11] screen printing,[12,13] gravure printing,[14,15] and flexographic printing[16] have been used for fabricating CNT thin-film transistors, which have great potential for applications in display electronics and sensing systems.[13,15,17−19] These methods eliminate the need of using a high-vacuum environment and multistage patterning process, thus paving the way for scalable manufacturing of large-area, low-cost, and flexible electronics.

Although the reported fully printed CNT TFTs[8,12−15,19,20] show satisfactory performance in terms of mobility and current on/off ratio, the channel lengths of such devices are rather large (>20 μm) due to the limitation of printing resolution and registration accuracy. Consequently, the on-state current densities of fully printed CNT TFTs in those papers are very low (on the scale between 10^{-1} μA/μm and 10^{-5} μA/μm). For example, our group published screen-printed CNT TFTs with 105 μm channel length and a current density of ~10^{-4} μA/μm.[12,13] Javey and Cho reported gravure-printed CNT TFTs with 85 μm channel length and a current density of ~1.4 × 10^{-4} μA/μm.[14,15] Inkjet and aerosol-jet printed CNT TFTs with ion-gel gating have also been reported with 25−100 μm channel length and an improved current density of ~10^{-1}-

Received: December 6, 2016
Accepted: January 24, 2017

DOI: 10.1021/acsnano.6b08185
ACS Nano XXXX, XXX, XXX−XXX

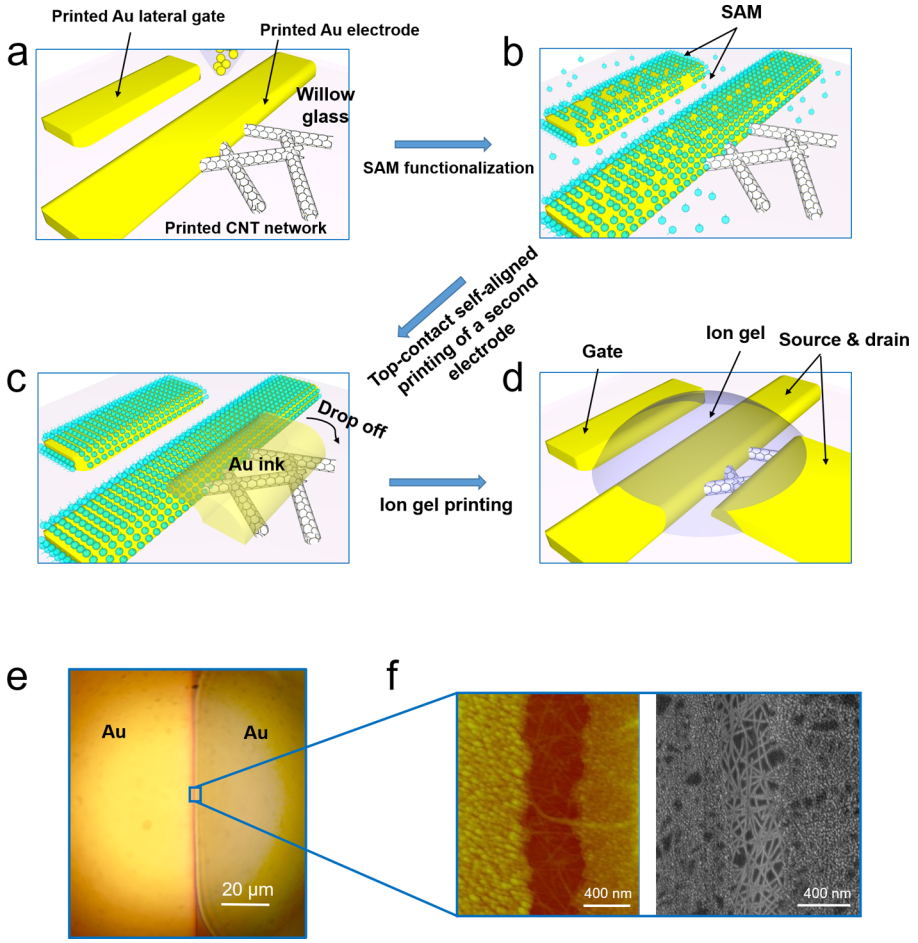

Figure 1. Top-contact self-aligned printed ultrashort channel CNT thin-film transistors. (a–d) Schematic diagrams showing the fabrication process of a top-contact self-aligned printed ultrashort channel nanotube transistor. Schematic diagrams showing (a) the inkjet printing process of the first electrode on top of the preprinted nanotube network; (b) the surface functionalization of the electrodes with a SAM; (c) the self-aligned inkjet printing process of the second electrode on the SAM-decorated surface of the first electrode before dewetting; and (d) the inkjet printing of ion-gel dielectric. (e) Optical microscope image showing two printed electrodes defined by a top-contact self-aligned printing technique and the ultrashort channel formed between these two electrodes. (f) AFM and SEM images showing an ultrashort channel of 400 nm with nanotubes between two printed electrodes formed by self-aligned printing.

$10^{-3}\mu A/\mu m$.[7,8,19–21] For one of the most significant applications - current driving for organic light emitting diodes, low on-state current density of driving TFTs is disadvantageous since a large channel width is needed to achieve desirable brightness of the integrated light-emitting devices, resulting in a low aspect ratio. Also, such long-channel TFTs have low speed and high operation voltage, which may limit their applications such as radio frequency transistors.[22] Overall, downscaling of fully printed CNT TFTs is necessary to further improve the performance and widen the potential applications for scalable manufacturing of large-area and low-cost electronics. Previously Sirringhaus's group pioneered a back-contact self-aligned printing (SAP) method to develop ultrashort-channel organic transistors.[22,23] However, due to the vulnerability of organic materials to high temperature required by sintering gold ink, the organic TFTs were configured by having the organic semiconductor layer on top of the printed electrodes, thus forming back contacts to the channel. This introduced a self-assembled monolayer (SAM) between the semiconductor and metal contacts. As a result, the contact resistance may increase remarkably. In addition, as the channel length is downscaled to a sub-micron scale, a small effective thickness of dielectric layer is required to have a strong gating on the short-channel devices.

Here we report a facile and highly reliable top-contact self-aligned printing strategy to fabricate fully inkjet printed, ultrashort-channel (sub-micron), and lateral-gate CNT TFTs on willow glass. In this study, we first printed the CNT network and then printed the electrodes to form top contacts with a sub-micron channel in between. Therefore, the gold electrodes were printed and sintered on the semiconducting CNT network and directly formed good ohmic contacts, eliminating the SAM which may cause a large contact resistance.[22] Furthermore, a high capacitance ion-gel material[24] has been employed as the dielectric material with an effective thickness of sub-nanometer scale provided by an electrical double layer.[25] Thus, we have further improved the on-state current density and lowered the operation voltage of our devices with the enhanced gating. The as-printed short-channel CNT TFTs show excellent performance with a superior average on-state current density (4.5 $\mu A/\mu m$) at low operation voltage of gate voltage (V_G)= −1.5 V and source−drain voltage (V_{DS}) = −0.1 V, outstanding mobility (15.03 $cm^2\ V^{-1}\ s^{-1}$), and high current on/off ratio (~10^5). Compared with previous fully printed CNT TFTs, we dramatically downscaled the printed TFTs from tens of micrometers to sub-microns in channel length and realized great improvement in current density by orders of

DOI: 10.1021/acsnano.6b08185
ACS Nano XXXX, XXX, XXX−XXX

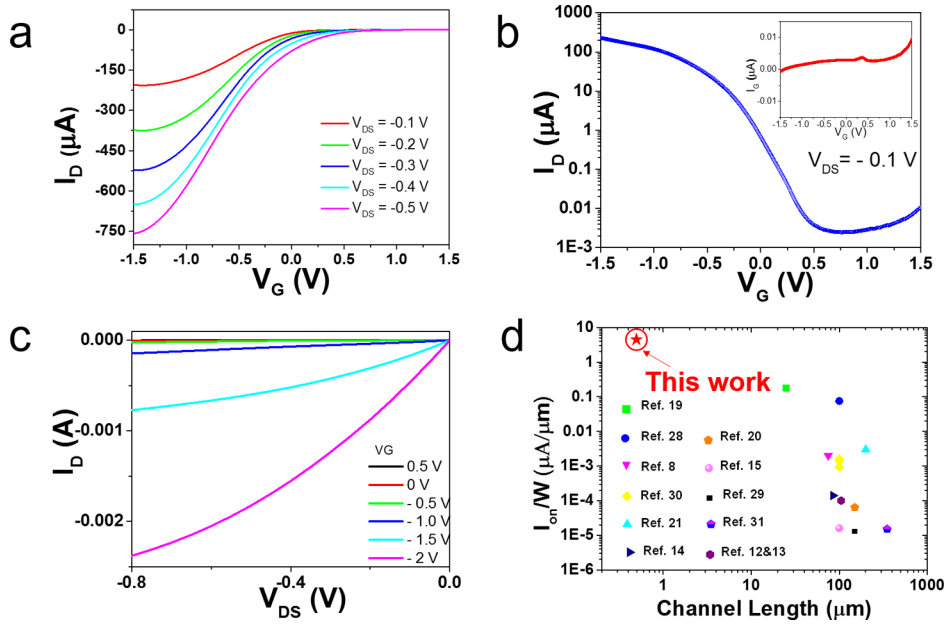

Figure 2. Electrical characterization of fully printed ultrashort channel CNT TFTs on willow glass. (a) Transfer characteristics (I_D−V_G) of a representative ultrashort channel nanotube TFT (L = 400 nm, W = 40 μm), measured at a different V_{DS}, from −0.1 V to −0.5 V with a step of −0.1 V. (b) Transfer characteristics measured under V_{DS} = −0.1 V showing a current on/off ratio of ∼1 × 10^5. The inset of this figure exhibits the gate leakage current as a function of V_G at V_{DS} = −0.1 V. (c) Output characteristic (I_D−V_D) of the same device measured at different V_G (from 0.5 V to −2 V with −0.5 V steps). (d) Comparison of channel length and on-state current density of printed CNT TFTs between this work and other work.

magnitude. We believe the advantageous performance will be highly desirable for future large-area high-definition printed displays, electronic skins, radio frequency applications, and sensing systems.

RESULTS AND DISCUSSION

Ultrashort channel CNT TFTs are printed on willow glass with lateral-gate device architecture and ion gel as the gate dielectric. In principle, any substrates which can go through the sintering temperature (∼250 °C) for gold (to be discussed below) can be used, such as Si/SiO_2 or glass substrate. Specifically, here we chose willow glass as our substrate for demonstration. As the first step, gold nanoparticle ink was printed as the lateral gate electrode, followed by sintering at 250 °C for 1 h. As the second step, a semiconducting-enriched SWCNT solution was printed and defined in the channel region. The printed nanotube film was then annealed in air at 200 °C to let the solvent evaporate. As previously reported,[26] annealing at 400 °C in vacuum can remove the excess polymer. However, this temperature may be too high for some potential substrates such as polyethylene terephthalate (PET) and, therefore, is not used here. The quality of the printed nanotube film was then inspected using field-emission scanning electron microscopy (FESEM), and the SEM image (Figure S1) shows the highly uniform clean nanotube random network. As the third step, the first gold electrode was printed to form a contact with the nanotube network (Figure 1a). After sintering in air for 1 h, SAM (1H,1H,2H,2H-perfluorodecanethiol (PFDT)) functionalization was performed to modify the surface of the printed gold electrodes to be hydrophobic (Figure 1b; details see Methods). Right after the treatment, the second gold electrode was initially printed in a partially overlapping fashion with the first electrode (Figure 1c). The gold ink landing on the surface of the SAM-decorated first electrode was repelled by the hydrophobic surface, and a sub-micron gap between the first electrode and the second electrode usually formed about 5 min after the printing and when the solvent was drying (Figure S2).[23,27] We have observed that with 5 min of slow drying in air after printing, the contact line of the second electrode, which initially overlapped slightly with the first electrode, retracted from the surface of the first electrode, leaving a color contrast at the location where the second electrode dewetted from (Figure S2a). The color contrast observed here may come from some residue of the ink solvent after the ink dewetted. The sample was then sintered at 220 °C in air for 1 h, which worked to remove surfactants from the printed gold particles and made the printed gold electrodes highly conductive. After sintering, the color contrast observed in Figure S2a disappeared completely (Figure S2b) due to solvent evaporation. The optical microscope image (Figure 1e) shows a sub-micron channel defined by the top-contact self-aligned printing, which was further characterized using atomic force microscopy (AFM) and FESEM. Figure 1f shows a well-defined channel of 400 nm with a CNT random network within the channel. The fabrication process of the device was completed with the printing of ion gel[24] as the gate dielectric (Figure 1d). Once the ion-gel droplet landed on the device, it spread out and formed a thin layer covering the channel region as well as the lateral gate. Thanks to the electrolytic gating nature of the ion gel,[24] lateral-gate device architecture can be used, which simplifies the printing process.

The electrical performance of the fully printed ultrashort channel CNT TFTs was studied and is shown in Figure 2. The transfer characteristics of a representative CNT TFT with channel length (L) = 400 nm and channel width (W) = 40 μm, measured under different drain voltages (V_{DS}) from −0.1 V to −0.5 V in a step of −0.1 V, are presented in Figure 2a, showing a typical p-type transistor behavior. Figure 2b exhibits the

DOI: 10.1021/acsnano.6b08185
ACS Nano XXXX, XXX, XXX−XXX

Table 1. Comparison of on-State Current Density for Printed CNT TFTs[a]

ref	L (μm)	method	dielectric	electrode	V_G (V)	V_{DS} (V)	I_{on}/W (μA/μm)	year
this work	0.496	inkjet	ion gel	Au	−1.5	−0.1	4.5	2016
28	100	inkjet	ion gel	Ag	−1	0.1	0.075	2008
8	75	inkjet	ion gel (PEI/$LiClO_4$)	Ag	1	0.5	0.002	2011
29	150	gravure + inkjet	BTO	Ag	−1.5	−0.1	0.000013	2011
21	200	inkjet	ion gel	metallic CNTs	−1.5	−0.1	0.003	2013
14	85	gravure	BTO+PMMA	Ag	−1.5	−0.1	0.00014	2013
12	105	screen	BTO	Ag	−1.5	−0.1	0.0001	2014
15	100	gravure	BTO	Ag	−1.5	−0.1	0.000016	2015
19	25	aerosol	ion gel	Au/PEDOT	−1.5	−0.1	0.18	2016
30	100	aerosol	SiO_2	Ag (double layer)	−1.5	−0.1	0.00094	2016
30	100	aerosol	SiO_2	metallic CNT	−1.5	−0.1	0.0014	2016
30	100	aerosol	SiO_2	Au	−1.5	−0.1	0.0016	2016
31	350	inkjet	polymer (PV3D3)	Ag	−1.5	−0.1	0.000015	2016
13	105	screen	BTO	Ag	−1.5	−0.1	0.0001	2016
20	150	inkjet	BTO/PDMS	unsorted CNTs	−1.5	−0.1	0.000064	2016

[a]If values were not provided in the manuscripts explicitly, they were estimated from the I−V curves presented in the manuscripts. The on-state current density of this work is the average value of 30 printed ultrashort channel CNT TFTs.

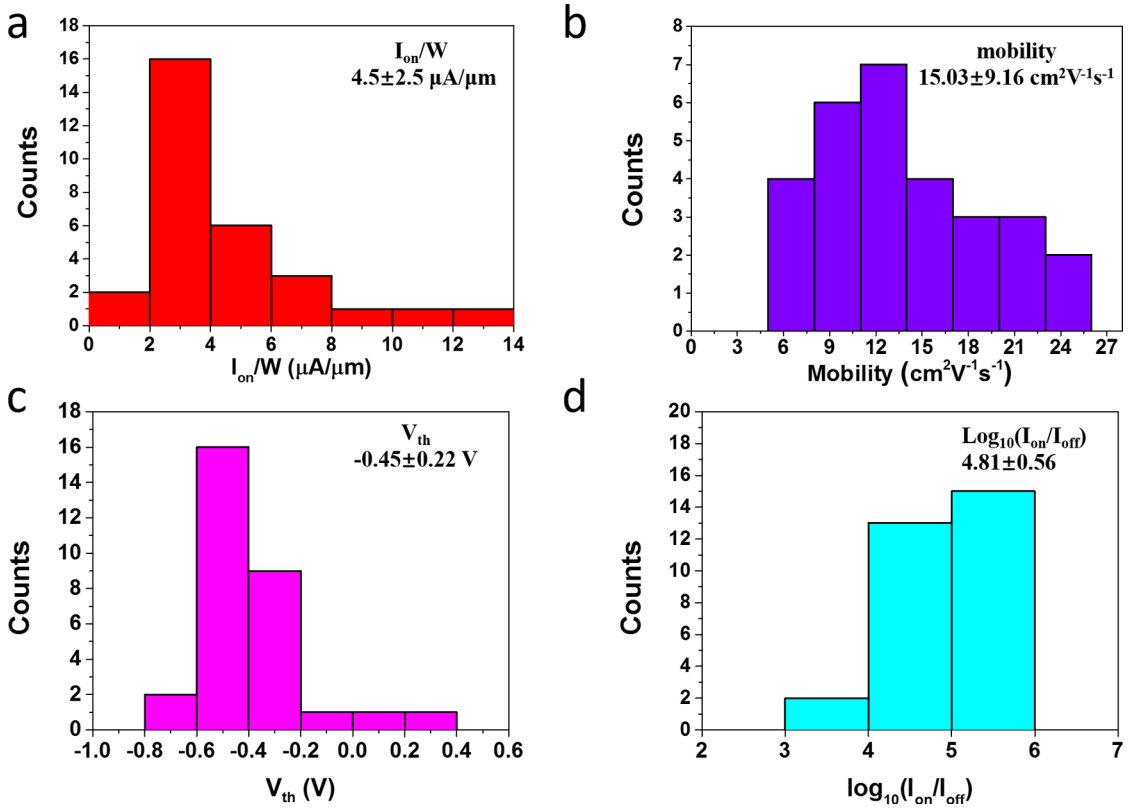

Figure 3. Statistics analysis of 30 CNT TFTs with L = 496 nm printed with top-contact self-aligned printing technique. (a) On-state current density distributions of 30 TFTs measured at V_G = −1.5 V and V_{DS} = −0.1 V. (b) Field-effect mobility distributions of 30 TFTs extracted from transfer characteristics measured at V_{DS} = −0.1 V. (c) Threshold voltage distributions of 30 TFTs. (d) Current on/off ratio distributions of 30 TFTs measured at V_{DS} = −0.1 V.

transfer curve of the representative device in logarithm scale under V_{DS} = −0.1 V, clearly showing a high current on/off ratio of ∼1 × 10^5. The threshold voltage of this TFT is ∼−0.2 V. Due to the high capacitance of the ion-gel gate dielectric, which is measured to be ∼1.5 μF/cm^2 at 100 Hz (Figure S3), the transistor can be operated with a gate voltage (V_G) of <−1.5 V and achieve a high on-state current density of 5.68 μA/μm at V_{DS} = −0.1 V. The average current density is 4.5 μA/μm, measured over 30 devices at V_G = −1.5 V and V_{DS} = −0.1 V. The field-effect mobility of this transistor is estimated to be 12.12 cm^2 V^{-1} s^{-1}, calculated with the standard linear regime relation, $I_D = \mu C_i \frac{W}{L}\left((V_{GS} - V_{th})V_{DS} - \frac{V_{DS}^2}{2}\right)$. Moreover, the gate leakage current as a function of gate voltage at V_{DS}= −0.1 V is shown in the inset of Figure 2b, indicating a small gate leakage current (<10 nA) for the ion-gel gate dielectric. The output characteristics of the same device (Figure 2c) show a typical current saturation for the p-type (hole) transport due to

DOI: 10.1021/acsnano.6b08185
ACS Nano XXXX, XXX, XXX−XXX

the pinch-off effect. The linear region of the output curve (Figure S4) indicates good ohmic contact between the printed gold electrodes and the printed nanotube network.

Our fully printed ultrashort channel CNT TFTs demonstrate a great success in downscaling the channel length of printed nanotube transistors from tens of micrometers to sub-microns. In consideration of the solution-based printing technique, we note that there is variation in the channel length within a single device and among different devices. We performed channel-length measurements of 9 devices with 15 different locations in each, as shown in Figure S5. The results show the channel length of self-aligned printed CNT TFTs is 496 ± 82 nm (Figure S5c,d). Our sub-micron nanotube TFTs show excellent electrical performance in terms of high on-state current density, low-voltage drive, outstanding on/off ratio, and good mobility. Especially, our printed ultrashort channel TFTs show a dramatically improved on-state current density of 4.5 μA/μm at V_{DS} = −0.1 V and V_G = −1.5 V, which is several orders of magnitude higher than other printed CNT TFTs. Figure 2d clearly shows the comparison of channel length and the on-state current density for printed CNT TFTs between this work and other previous reported works.[8,12−15,19−21,28−32] From Figure 2d, we can observe that our printed CNT TFTs have the shortest channel length and the highest on-state current density at a low drain voltage of −0.1 V and a small gate voltage of −1.5 V. Detailed comparison of all the representative printed CNT TFTs reported so far has been presented in Table 1, including the printing method, gate dielectric material, metal contact, on-state current density, *etc*. Based on Table 1, we can also conclude that our fully printed CNT TFTs have the smallest channel length and the best on-state current density. The ultrashort channel length may enable scaling up the number of transistors per unit area, which may be promising for applications such as printed CNT TFT active backplanes for high-resolution sensing, display, *etc*. Moreover, the high current density at low-voltage operations makes these printed CNT TFTs good candidates for display applications and low-power-consumption portable electronics.

In order to assess the uniformity of the fully printed ultrashort channel CNT TFTs, 30 transistors with a channel length of ∼496 nm have been printed, and the electrical performance has been tested. Statistics studies of the key device parameters, including the on-state current density, field-effect mobility, threshold voltage, and the current on/off ratio, of the 30 printed transistors have been conducted and presented in Figure 3. Judging from the on-state current density distributions of the 30 printed CNT TFTs (Figure 3a), these devices show good uniformity with an on-state current density of 4.5 ± 2.5 μA/μm at V_{DS} = −0.1 V and V_G = −1.5 V. We note that while the variation in channel length affects the variation in the on-current, it does not fully account for the on-current variation, as the variation in the CNT density can be another important factor. Field-effect charge carrier mobilities of the 30 printed TFTs are extracted from the transfer curves measured at V_{DS} = −0.1 V. The statistic distributions of mobilities are shown in Figure 3b, illustrating uniform mobility with an average value of 15.03 cm^2 V^{-1} s^{-1}. Moreover, the transistors have threshold voltages of −0.45 ± 0.22 V (Figure 3c). Furthermore, Figure 3d shows the distribution of current on/off ratios, with $\log_{10}(I_{on}/I_{off})$ of 4.81 ± 0.56, which is comparable with previously published ion-gel-gated CNT TFT work.[10] The semiconducting nanotube ink was purchased from Nanointegris Inc. with ultrahigh purity of >99.99%, which is believed to be the reason for the observed high on/off ratio >10^4. As a result, even if 1 out of 10000 nanotubes is metallic, we should be able to obtain high on/off ratio. Overall, printing of ultrashort channel CNT TFTs with self-aligned printing approach is highly reliable and reproducible, and all of the printed sub-micron nanotube TFTs show highly uniform electrical performance.

In order to fully reveal the benefits of channel length downscaling, systematic comparison was carried out between the printed CNT TFTs with 496 nm channel length and TFTs with channel lengths of 40, 120, and 150 μm. A control group of 15 CNT TFTs was printed with channel lengths of 40, 120, and 150 μm (Figure S6), following the same printing procedure as for short channel devices. All of the printed TFTs with long channel lengths were electrically tested with exactly the same measurement parameters of the short channel devices, and the comparison was made and is presented in Figure 4a,b. Transfer characteristics of four representative CNT TFTs, with channel

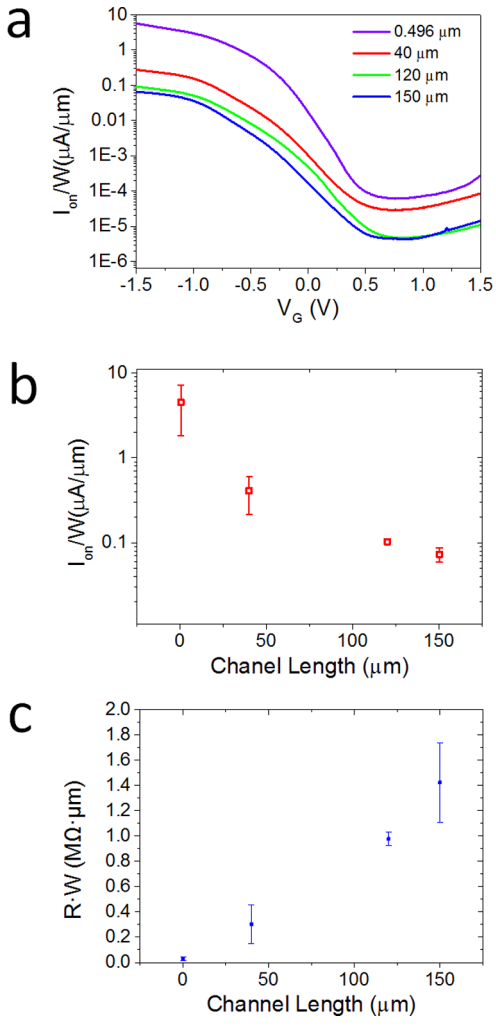

Figure 4. Electrical characterization of printed CNT TFTs with different channel lengths. (a) Transfer characteristics of representative printed CNT TFTs with channel lengths of 496 nm (violet), 40 μm (red), 120 μm (green), and 150 μm (blue). (b) Statistical study of 45 printed CNT TFTs showing an on-state current density as a function of channel length. (c) Statistical study of 45 printed CNT TFTs showing width-normalized total resistance as a function of channel length.

DOI: 10.1021/acsnano.6b08185
ACS Nano XXXX, XXX, XXX−XXX

lengths of 496 nm, 40 μm, 120 μm, and 150 μm, are shown in Figure 4a, indicating a much higher on-state current density for the 496 nm CNT transistor compared to transistors with longer channel lengths. Figure 4b further shows the on-state current density of these printed transistors as a function of the channel length, exhibiting a decreasing trend of the on-state current density as the channel length increases. Moreover, the width-normalized total resistance ($R{\cdot}W$) of CNT TFTs as a function of channel length is exhibited in Figure 4c. As channel length scales from 496 nm to 40, 120, and 150 μm, the $R{\cdot}W$ increases by a factor of 10, 34 and 50, respectively. Overall, the printed ultrashort channel CNT TFTs show a remarkably high on-state current density at a low-voltage operation, which makes it promising for low power consumption displays and portable electronics.

By now, we have talked about the printing of CNT TFTs with sub-micron channel length using a top-contact self-aligned printing strategy. For future work, tunable channel length and channel width may be highly desirable for wide applications. The channel length of TFTs defined by the self-aligned printing technique is mainly determined by the repulsion force between the metal nanoparticle ink and the SAM-modified first electrode. Many factors can be adjusted to tune the channel length. First of all, by choosing different thiol-based SAMs, the surface hydrophobicity of the first electrode can be altered, and different channel lengths can be achieved. Second, the concentration of the SAM and the functionalization time may affect the hydrophobicity of the electrode surface and yield different channel lengths. Moreover, the viscosity of the metal nanoparticle ink can also be tuned to achieve the desirable channel length. The channel width of the printed TFTs is basically controlled by the printing process, which can be varied in a range from 20 to 1000 μm. In addition, many different kinds of ion gels[25] have been reported so far and can be used as the gate dielectric in replacement of the ion gel we used in this paper for the self-aligned printed transistors. Furthermore, the dielectric materials for the top-contact self-aligned printed TFTs are not limited to ion gel. Indeed, the top-contact self-aligned printing technique is compatible with various state-of-the-art dielectric deposition technologies. Many dielectric materials can be deposited as the gate dielectric layer. For example, a thin layer (~20 nm) of atomic layer deposition (ALD)-deposited aluminum oxide can be a great alterative dielectric material for the self-aligned printed TFTs. Last but not least, the top-contact self-aligned printing technique is not limited to CNT TFTs. Instead, a wide range of channel materials, such as two-dimensional transition-metal dichalcogenide monolayers, organic materials (which can be stable up to 200–280 °C), *etc.*, are compatible with this printing strategy and are worth exploration.

CONCLUSION

In conclusion, we have successfully downscaled the channel length of fully printed CNT TFTs to a sub-micron level with a top-contact self-aligned printing technique, which bypassed the resolution limit of inkjet printing technology. In addition, high-capacitance ion gel has been printed as the gate dielectric to further promote the on-state current density at low-voltage operation. Notably, the fully printed sub-micron CNT TFTs exhibit superior electrical performance, with an outstanding average on-state current density of 4.5 μA/μm at V_G = −1.5 V and V_{DS} = −0.1 V, large average carrier mobility of 15.03 cm^2 V^{-1} s^{-1}, and high current on/off ratio of ~1 × 10^5. Especially, our printed ultrashort channel CNT TFTs demonstrate a huge improvement in terms of on-state current density, which is several orders of magnitude higher than previously reported printed CNT TFTs.[8,12−15,19−21,28−32] The successful channel-length downscaling and on-state current improvement make printed ultrashort-channel CNT TFTs a capable candidate as a low-cost, high-definition solution for display electronics, sensing systems, electronic skins, *etc.*

METHODS

Printing of Lateral Gate Electrodes. Willow glass with a thickness of 200 μm was used as the substrate. Before printing, acetone sonication and isopropyl alcohol (IPA) rinsing were performed as surface cleaning steps. Gold nanoparticle ink (UTDAu40IJ, UT Dots, Inc.), with 40% gold nanoparticles dispersed in a hydrocarbon solvent, was printed using a SonoPlot printer (Microplotter Desktop, SonoPlot, Inc.) with a 50 μm glass nozzle. After printing, the printed gold ink was sintered in air at 250 °C for 1 h.

Printing of CNT Channels. A semiconducting-enriched SWCNT solution (IsoSol-S100, NanoIntegris, Inc.) was defined in the channel region with a SonoPlot printer, followed by baking in air at 200 °C for 1 h. The quality of the printed CNT random network was examined using a FESEM (Hitachi S4800).

Printing of First Contact Electrodes. The first gold contact electrodes were printed on top of the printed CNT film using the same printing conditions as the gate electrode, followed by a 1 h sintering at 220 °C in air. A slightly reduced sintering temperature was used to avoid damaging the printed CNTs.

Self-Aligned Printing of Second Contact Electrodes. First, the surface of the printed gold electrodes was modified with a SAM, 1H,1H,2H,2H-perfluorodecanethiol (PFDT) (97%, Sigma-Aldrich). Specifically, the sample was immersed in an IPA-diluted PFDT solution with a dilution ratio of 1:10 and was treated for 18 h, followed by IPA rinsing and nitrogen blow-drying. After the surface functionalization, xylene-diluted gold nanoparticle ink (gold ink:xylene =1:2) was printed on the PFDT-treated surface of the first gold electrodes with a slight overlap. After the gold ink landed on the SAM-modified first electrode surface, it eventually dewetted from the surface under repulsion force. After 5 min of slow drying in air, a sub-micron gap between the two electrodes was observed under an optical microscope. Then the printed second electrodes were sintered on a hot plate at 220 °C for 1 h. Optical microscope, AFM, and SEM were used to characterize the channel length.

Printing of Ion-Gel Gate Dielectric. Ion-gel ink was formulated by mixing a biblock copolymer of poly(styrene-*block*-methyl methacrylate) (Sigma-Aldrich), an ionic liquid of 1-ethyl-3-methyl-imidazolium bis(trifluoromethylsulfonyl)imide (EMD Chemicals), and *n*-butyl acetate (Sigma-Aldrich) in a ratio of 2:9:90 in weight. SonoPlot printer with a nozzle of 70 μm was used to drop the ion gel on the device region covering the channel and the lateral gate.

ASSOCIATED CONTENT

Supporting Information

The Supporting Information is available free of charge on the ACS Publications website at DOI: 10.1021/acsnano.6b08185.

Additional experimental details and data (PDF)

AUTHOR INFORMATION

Corresponding Author

*E-mail: chongwuz@usc.edu.

ORCID

Yihang Liu: 0000-0002-2491-9439

Chongwu Zhou: 0000-0001-8448-8450

Present Address

[§]These authors contributed equally.

DOI: 10.1021/acsnano.6b08185
ACS Nano XXXX, XXX, XXX−XXX

Notes

The authors declare no competing financial interest.

ACKNOWLEDGMENTS

We would like to acknowledge the collaboration of this research with King Abdul-Aziz City for Science and Technology (KACST) *via* The Center of Excellence for Nanotechnologies (CEGN).

REFERENCES

(1) Cao, Q.; Kim, H. S.; Pimparkar, N.; Kulkarni, J. P.; Wang, C. J.; Shim, M.; Roy, K.; Alam, M. A.; Rogers, J. A. Medium-Scale Carbon Nanotube Thin-Film Integrated Circuits on Flexible Plastic Substrates. *Nature* **2008**, *454*, 495−500.

(2) Park, J. U.; Hardy, M.; Kang, S. J.; Barton, K.; Adair, K.; Mukhopadhyay, D. K.; Lee, C. Y.; Strano, M. S.; Alleyne, A. G.; Georgiadis, J. G.; Ferreira, P. M.; Rogers, J. A. High-Resolution Electrohydrodynamic Jet Printing. *Nat. Mater.* **2007**, *6*, 782−789.

(3) Sun, D. M.; Timmermans, M. Y.; Tian, Y.; Nasibulin, A. G.; Kauppinen, E. I.; Kishimoto, S.; Mizutani, T.; Ohno, Y. Flexible High-Performance Carbon Nanotube Integrated Circuits. *Nat. Nanotechnol.* **2011**, *6*, 156−161.

(4) Wang, C.; Hwang, D.; Yu, Z.; Takei, K.; Park, J.; Chen, T.; Ma, B.; Javey, A. User-Interactive Electronic Skin for Instantaneous Pressure Visualization. *Nat. Mater.* **2013**, *12*, 899−904.

(5) Wang, C.; Takei, K.; Takahashi, T.; Javey, A. Carbon Nanotube Electronics - Moving Forward. *Chem. Soc. Rev.* **2013**, *42*, 2592−2609.

(6) Wang, C.; Zhang, J. L.; Ryu, K. M.; Badmaev, A.; De Arco, L. G.; Zhou, C. W. Wafer-Scale Fabrication of Separated Carbon Nanotube Thin-Film Transistors for Display Applications. *Nano Lett.* **2009**, *9*, 4285−4291.

(7) Cai, L.; Zhang, S.; Miao, J.; Yu, Z.; Wang, C. Fully Printed Foldable Integrated Logic Gates with Tunable Performance Using Semiconducting Carbon Nanotubes. *Adv. Funct. Mater.* **2015**, *25*, 5698−5705.

(8) Chen, P. C.; Fu, Y.; Aminirad, R.; Wang, C.; Zhang, J. L.; Wang, K.; Galatsis, K.; Zhou, C. W. Fully Printed Separated Carbon Nanotube Thin Film Transistor Circuits and Its Application in Organic Light Emitting Diode Control. *Nano Lett.* **2011**, *11*, 5301−5308.

(9) Ha, M.; Xia, Y.; Green, A. A.; Zhang, W.; Renn, M. J.; Kim, C. H.; Hersam, M. C.; Frisbie, C. D. Printed, Sub-3V Digital Circuits on Plastic from Aqueous Carbon Nanotube Inks. *ACS Nano* **2010**, *4*, 4388−4395.

(10) Ha, M. J.; Seo, J. W. T.; Prabhumirashi, P. L.; Zhang, W.; Geier, M. L.; Renn, M. J.; Kim, C. H.; Hersam, M. C.; Frisbie, C. D. Aerosol Jet Printed, Low Voltage, Electrolyte Gated Carbon Nanotube Ring Oscillators with Sub-5 μs Stage Delays. *Nano Lett.* **2013**, *13*, 954−960.

(11) Kim, B.; Jang, S.; Geier, M. L.; Prabhumirashi, P. L.; Hersam, M. C.; Dodabalapur, A. High-Speed, Inkjet-Printed Carbon Nanotube/Zinc Tin Oxide Hybrid Complementary Ring Oscillators. *Nano Lett.* **2014**, *14*, 3683−3687.

(12) Cao, X.; Chen, H. T.; Gu, X. F.; Liu, B. L.; Wang, W. L.; Cao, Y.; Wu, F. Q.; Zhou, C. W. Screen Printing as a Scalable and Low-Cost Approach for Rigid and Flexible Thin-Film Transistors Using Separated Carbon Nanotubes. *ACS Nano* **2014**, *8*, 12769−12776.

(13) Cao, X.; Lau, C.; Liu, Y.; Wu, F.; Gui, H.; Liu, Q.; Ma, Y.; Wan, H.; Amer, M. R.; Zhou, C. W. Fully Screen-Printed, Large-Area, and Flexible Active-Matrix Electrochromic Displays Using Carbon Nanotube Thin-Film Transistors. *ACS Nano* **2016**, *10*, 9816−9822.

(14) Lau, P. H.; Takei, K.; Wang, C.; Ju, Y.; Kim, J.; Yu, Z.; Takahashi, T.; Cho, G.; Javey, A. Fully Printed, High Performance Carbon Nanotube Thin-Film Transistors on Flexible Substrates. *Nano Lett.* **2013**, *13*, 3864−3869.

(15) Yeom, C.; Chen, K.; Kiriya, D.; Yu, Z.; Cho, G.; Javey, A. Large-Area Compliant Tactile Sensors Using Printed Carbon Nanotube Active-Matrix Backplanes. *Adv. Mater.* **2015**, *27*, 1561−1566.

(16) Higuchi, K.; Kishimoto, S.; Nakajima, Y.; Tomura, T.; Takesue, M.; Hata, K.; Kauppinen, E. I.; Ohno, Y. High-Mobility, Flexible Carbon Nanotube Thin-Film Transistors Fabricated by Transfer and High-Speed Flexographic Printing Techniques. *Appl. Phys. Express* **2013**, *6*, 085101.

(17) Zhang, J. L.; Fu, Y.; Wang, C.; Chen, P. C.; Liu, Z. W.; Wei, W.; Wu, C.; Thompson, M. E.; Zhou, C. W. Separated Carbon Nanotube Macroelectronics for Active Matrix Organic Light-Emitting Diode Displays. *Nano Lett.* **2011**, *11*, 4852−4858.

(18) Xu, W.; Zhao, J.; Qian, L.; Han, X.; Wu, L.; Wu, W.; Song, M.; Zhou, L.; Su, W.; Wang, C.; Nie, S.; Cui, Z. Sorting of Large-Diameter Semiconducting Carbon Nanotube and Printed Flexible Driving Circuit for Organic Light Emitting Diode (OLED). *Nanoscale* **2014**, *6*, 1589−1595.

(19) Li, H.; Tang, Y.; Guo, W.; Liu, H.; Zhou, L.; Smolinski, N. Polyfluorinated Electrolyte for Fully Printed Carbon Nanotube Electronics. *Adv. Funct. Mater.* **2016**, *26*, 6914−6920.

(20) Cai, L.; Zhang, S.; Miao, J.; Yu, Z.; Wang, C. Fully Printed Stretchable Thin-Film Transistors and Integrated Logic Circuits. *ACS Nano* **2016**, *10*, 11459.

(21) Sajed, F.; Rutherglen, C. All-Printed and Transparent Single Walled Carbon Nanotube Thin Film Transistor Devices. *Appl. Phys. Lett.* **2013**, *103*, 143303.

(22) Noh, Y. Y.; Zhao, N.; Caironi, M.; Sirringhaus, H. Downscaling of Self-Aligned, All-Printed Polymer Thin-Film Transistors. *Nat. Nanotechnol.* **2007**, *2*, 784−789.

(23) Caironi, M.; Gili, E.; Sakanoue, T.; Cheng, X. Y.; Sirringhaus, H. High Yield, Single Droplet Electrode Arrays for Nanoscale Printed Electronics. *ACS Nano* **2010**, *4*, 1451−1456.

(24) Hyun, W. J.; Secor, E. B.; Rojas, G. A.; Hersam, M. C.; Francis, L. F.; Frisbie, C. D. All-Printed, Foldable Organic Thin-Film Transistors on Glassine Paper. *Adv. Mater.* **2015**, *27*, 7058−7064.

(25) Kim, S. H.; Hong, K.; Xie, W.; Lee, K. H.; Zhang, S. P.; Lodge, T. P.; Frisbie, C. D. Electrolyte-Gated Transistors for Organic and Printed Electronics. *Adv. Mater.* **2013**, *25*, 1822−1846.

(26) Brady, G. J.; Way, A. J.; Safron, N. S.; Evensen, H. T.; Gopalan, P.; Arnold, M. S. Quasi-ballistic carbon nanotube array transistors with current density exceeding Si and GaAs. *Sci. Adv.* **2016**, *2*, e1601240.

(27) Zhao, N.; Chiesa, M.; Sirringhaus, H.; Li, Y. N.; Wu, Y. L. Self-Aligned Inkjet Printing of Highly Conducting Gold Electrodes with Submicron Resolution. *J. Appl. Phys.* **2007**, *101*, 064513.

(28) Vaillancourt, J.; Zhang, H. Y.; Vasinajindakaw, P.; Xia, H. T.; Lu, X. J.; Han, X. L.; Janzen, D. C.; Shih, W. S.; Jones, C. S.; Stroder, M.; Chen, M. Y. H.; Subbaraman, H.; Chen, R. T.; Berger, U.; Renn, M. All Ink-Jet-Printed Carbon Nanotube Thin-Film Transistor on a Polyimide Substrate with an Ultrahigh Operating Frequency of over 5 GHz. *Appl. Phys. Lett.* **2008**, *93*, 243301.

(29) Noh, J.; Jung, M.; Jung, K.; Lee, G.; Lim, S.; Kim, D.; Kim, S.; Tour, J. M.; Cho, G. Integrable Single Walled Carbon Nanotube (SWNT) Network Based Thin Film Transistors Using Roll-to-Roll Gravure and Inkjet. *Org. Electron.* **2011**, *12*, 2185−2191.

(30) Cao, C. Y.; Andrews, J. B.; Kumar, A.; Franklin, A. D. Improving Contact Interfaces in Fully Printed Carbon Nanotube Thin-Film Transistors. *ACS Nano* **2016**, *10*, 5221−5229.

(31) Lee, D.; Yoon, J.; Lee, J.; Lee, B. H.; Seol, M. L.; Bae, H.; Jeon, S. B.; Seong, H.; Im, S. G.; Choi, S. J.; Choi, Y. K. Logic Circuits Composed of Flexible Carbon Nanotube Thin-Film Transistor and Ultra-Thin Polymer Gate Dielectric. *Sci. Rep.* **2016**, *6*, 26121.

(32) Vuttipittayamongkol, P.; Wu, F. Q.; Chen, H. T.; Cao, X.; Liu, B. L.; Zhou, C. W. Threshold Voltage Tuning and Printed Complementary Transistors and Inverters Based on Thin Films of Carbon Nanotubes and Indium Zinc Oxide. *Nano Res.* **2015**, *8*, 1159−1168.

DOI: 10.1021/acsnano.6b08185
ACS Nano XXXX, XXX, XXX−XXX